Journal of Alloys and Compounds 506 (2010) 626–630

Contents lists available at ScienceDirect

Journal of Alloys and Compounds

journal homepage: www.elsevier.com/locate/jallcom

Magnetic properties and magnetocaloric effect in $Dy_{1-x}Sc_xNi_2$ solid solutions

J. Ćwik[a,b,*], T. Palewski[a], K. Nenkov[a,b], J. Lyubina[b], O. Gutfleisch[b], J. Klamut[a,c]

[a] International Laboratory of High Magnetic Fields and Low Temperatures, Gajowicka 95, 53-421 Wroclaw, Poland
[b] IFW Dresden, Institute of Metallic Materials, Postfach 270016, 01171 Dresden, Germany
[c] Institute of Low Temperature and Structure Research, PAS, Okolna 2, 50-422 Wroclaw, Poland

ARTICLE INFO

Article history:
Received 14 April 2010
Received in revised form 28 June 2010
Accepted 30 June 2010
Available online 19 August 2010

Keywords:
Rare earth alloys and compounds
Magnetically ordered materials
Heat capacity
Magentisation
Magnetocaloric

ABSTRACT

X-ray diffraction, magnetization, magnetic susceptibility, and heat capacity data are reported for the solid solutions $Dy_{1-x}Sc_xNi_2$ ($0 \le x \ge 1$). All the $Dy_{1-x}Sc_xNi_2$ solid solutions are single phase with the C15 cubic Laves phase superstructure. The alloys with $x \le 0.8$ are ferromagnets with a low (below 22 K) Curie temperature that decreases from 21.1 K for $DyNi_2$ to 4.5 K for $Dy_{0.2}Sc_{0.8}Ni_2$. $Dy_{0.1}Sc_{0.9}Ni_2$ and $ScNi_2$ have no long-range magnetic order down to 2 K. At high temperatures, all the $Dy_{1-x}Sc_xNi_2$ solid solutions, except $ScNi_2$, are Curie–Weiss paramagnets. The Debye temperature, phonon and conduction electron contributions as well as a magnetic contribution to the heat capacity have been determined from heat capacity measurements. The magnetocaloric effect for selected solid solutions was determined in magnetic fields up to 3 T.

1. Introduction

Intermetallic compounds formed between rare earths (R) and 3d transition metals (M) have attracted considerable attention owing to their potential for various applications such as permanent magnets, magneto-optical recording and magneto-acoustic materials. Recently, there has been a vigorous activity in the development of magnetocaloric materials, which are the active materials in magnetic refrigerators [1–10]. The magnetocaloric effect (MCE) manifests itself as the isothermal magnetic entropy change, ΔS_M, or as the adiabatic temperature change, ΔT_{ad}, of a magnetic material when exposed to a magnetic field. The magnetic properties of RNi_2 compounds have been extensively studied [11]. According to earlier magnetic measurements [12], the magnetism of the RNi_2 compounds comes from the unfilled 4f R-shell, since the Ni ions are practically nonmagnetic. However, conduction electrons of the Ni ions participate in indirect exchange interaction among the localized R-magnetic moment and some authors [13,14] reported the possible existence of the residual magnetic moment at the nickel atoms. Along with the exchange interaction usually considered in the molecular field approximation, the coupling of magnetic ions with the external magnetic field and the cubic crystal electric field (CEF) constitutes an appropriated framework to describe the magnetic behavior of RNi_2. Moreover, the existing exchange interactions between the localized 4f magnetic moments (via the conduction electrons) produce the magnetic order at low temperatures. A ferromagnetic order and relatively low Curie temperature are observed in $DyNi_2$. The ordering temperatures, reported in the literature scatter considerably from 21 to 32 K [15–17]. The magnetic susceptibility of $ScNi_2$ and its temperature dependence show that this compound is characterized by the Pauli paramagnetism [18].

The first crystallographic data on the RNi_2 compounds suggests that all these compounds crystallize in the cubic C15 structure [19]. However, in 1993, Latroche et al. [20] showed that $TbNi_2$ as well as most of the other RNi_2 compounds crystallize in a cubic structure with regularly arranged vacancies on the rare earth sites forming a superstructure (space group $F\bar{4}3m$) of the cubic Laves phase with cell parameters twice as large as the lattice parameter of the RNi_2 Laves phase. The formation of the superstructure with ordered vacancies at the R sites is energetically favourable; this has been confirmed by ab initio total energy calculations [21].

The purpose of this work is to study and analyze physical properties of $Dy_{1-x}Sc_xNi_2$ solid solutions upon substitution of Dy atoms by Sc atoms and the study of their magnetocaloric properties.

2. Experimental

Polycrystalline samples of $Dy_{1-x}Sc_xNi_2$ ($0 \le x \le 1$) solid solutions were prepared by arc-melting stoichiometric proportions of starting materials (of at least 99.9% purity) on a water-cooled copper crucible under high purity argon atmosphere. The alloys were re-melted four times to ensure good homogeneity. The mass losses after the melting were less than 1 wt%. The buttons were wrapped in a tantalum foil, sealed in an evacuated quartz ampoule, and annealed at 850 °C for 2 weeks.

* Corresponding author at: International Laboratory of High Magnetic Fields and Low Temperatures, Gajowicka 95, 53-421 Wroclaw, Poland.
E-mail address: cwikjac@ml.pan.wroc.pl (J. Ćwik).

0925-8388/$ – see front matter © 2010 Elsevier B.V. All rights reserved.
doi:10.1016/j.jallcom.2010.06.192

The crystal structure and the phase purity of the samples were analyzed using Rietveld refinement of X-ray diffraction data. Magnetization measurements, in the temperature range of 4.2–200 K, were carried out using vibrating sample magnetometer with a step motor in applied fields up to 14 T using a Bitter-type magnet. The heat capacity was measured using Quantum Design PPMS 14 Heat Capacity System in a temperature range of 2–295 K without magnetic field and in a magnetic field of 1, 2 and 3 T.

3. Results and discussion

3.1. Structural investigation

The Rietveld refinement of X-ray powder diffraction data revealed that the polycrystalline $Dy_{1-x}Sc_xNi_2$ solid solutions are single phase and have the cubic C15 superstructure (space group $F\bar{4}3m$). Only in the case of $Dy_{0.9}Sc_{0.1}Ni_2$ a small amount (0.3 %) of Dy_2O_3 as impurity phase has been detected. In the refinement, Sc was supposed to partially occupy Dy sites only (the atomic form factors of Ni and Sc vary only marginally). The partitioning of Sc atoms on Dy sites accounted well for varying diffraction peak intensities. The lattice parameters obtained from the refinement gives the values equal 1.429 nm for $Dy_{0.9}Sc_{0.1}Ni_2$ and 1.395 nm for the $Dy_{0.1}Sc_{0.9}Ni_2$. The substitution of scandium for dysprosium in the $Dy_{1-x}Sc_xNi_2$ solid solutions leads to the decrease of the lattice parameter; this dependence is largely linear.

3.2. Magnetization

The principal magnetic parameters of the investigated samples are listed in Table 1. The solid solutions with $x \leq 0.8$ are characterized by a ferromagnetic order and relatively low Curie temperatures, below 22 K. The magnetization curves measured at 4.2 K for these samples with various scandium contents are presented in Fig. 1. In the case of parent compound $DyNi_2$ a small hysteresis loop in the low magnetic field is observed. Saturation is not reached even in the maximum applied magnetic fields of 14 T. Values of the saturation magnetic moment per dysprosium atom were determined from the magnetization corresponding to a magnetic field of 14 T by extrapolation to $\mu_o H = 0$. The μ_S values are well below $gJ = 10\ \mu_B$, which is expected for an assembly of free Dy^{3+} ions (Table 1). The difference between the expected and the experimental μ_S values is the lowest in $DyNi_2$ ($1.25\ \mu_B$) and the highest in the case of $Dy_{0.2}Sc_{0.8}Ni_2$ ($2.8\ \mu_B$). The large a deviations could be a consequence of the nickel atom having a magnetic moment antiparallel to the dysprosium one [22] and/or due to a negative polarization of conduction band electrons [23]. If the first suggestion is true, the experimental values of ordered magnetic moment keep up assumption that Ni atoms carry magnetic moment in these solid solutions. For all solid solutions, we observe the decrease of the saturation magnetic moment with increasing Sc content; in the case of $Dy_{0.2}Sc_{0.8}Ni_2$ it is $\mu_S = 7.2\ \mu_B$/Dy atom.

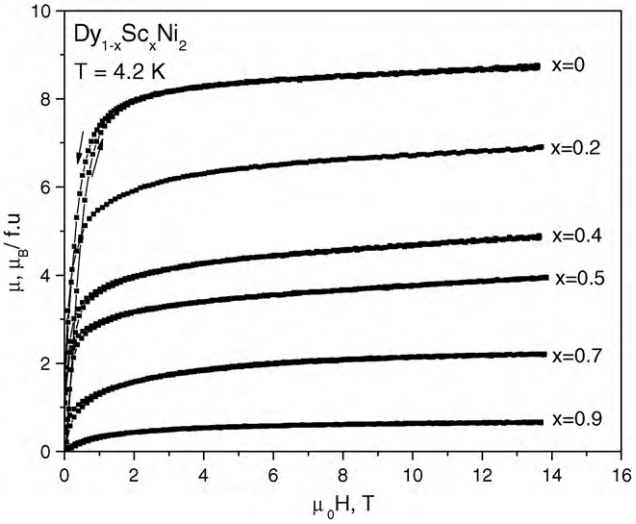

Fig. 1. Magnetization curves measured at 4.2 K for the $Dy_{1-x}Sc_xNi_2$ ($x = 0$, 0.2, 0.4, 0.5, 0.7 and 0.9) solid solutions.

3.3. Magnetic susceptibility

The temperature dependence of the magnetic susceptibility measured at low temperature ($T \leq 50$ K) near the magnetic ordering temperature in a static magnetic field of 0.5 T for all the studied solid solutions is shown in Fig. 2. It is seen that all solid solutions are magnetically ordered below 22 K and with increasing the Sc content their magnetic susceptibility and ordering temperature decrease. The temperature dependence of the inverse magnetic susceptibility for all the investigated solid solutions in the paramagnetic state obeys the Curie–Weiss law. The paramagnetic Curie temperature Θ_P and the effective magnetic moment μ_{eff} were determined using the Curie–Weiss law. The Θ_P values decrease monotonously as the scandium content increases and for the solid solution with $x = 0.8$ there is $\Theta_P = 2.5$ K (see Table 1). The values of Θ_P for solid solution with $x \leq 0.6$ are larger than the T_C values. Probably some ferromagnetic impurities may introduce a deviation on the C–W fit. The magnetic susceptibility of $ScNi_2$ is characterized by a very weak temperature dependence that is close to the

Table 1
Magnetic properties and cell parameter of $Dy_{1-x}Sc_xNi_2$ solid solutions. μ_S is the saturation magnetic moment, μ_B/Dy is the saturation magnetic moment per dysprosium atom, T_C is the Curie temperature, Θ_P is the paramagnetic Curie temperature, μ_{eff} is effective magnetic moment, μ_B/Dy is effective magnetic moment per dysprosium atom. All the data have been obtained from magnetic measurements.

Compound	Ordered state			Paramagnetic state		Cell parameters
	μ_S (μ_B) T = 4.2 K; $\mu_o H$ = 14 T		T_C	Θ_P	μ_{eff} (($_B$) $\mu_o H$ = 0.5 T	a
	(μ_B/f.u.)	(μ_B/Dy)	(K)	(K)	(μ_B/Dy)	(nm)
$DyNi_2$	8.75	8.75	21.3	25.7	10.5	1.432
$Dy_{0.9}Sc_{0.1}Ni_2$	7.57	8.41	20.1	24.3	9.4	1.429
$Dy_{0.8}Sc_{0.2}Ni_2$	6.91	8.64	17.2	23.4	8.6	1.425
$Dy_{0.7}Sc_{0.3}Ni_2$	5.80	8.29	16.3	18.1	8.8	1.422
$Dy_{0.6}Sc_{0.4}Ni_2$	4.88	8.13	13.5	15.6	9.6	1.416
$Dy_{0.5}Sc_{0.5}Ni_2$	3.96	7.92	10.8	11.5	10.2	1.409
$Dy_{0.4}Sc_{0.6}Ni_2$	3.11	7.78	6.4	8	9.6	1.404
$Dy_{0.3}Sc_{0.7}Ni_2$	2.23	7.43	5.1	4.4	9.5	1.399
$Dy_{0.2}Sc_{0.8}Ni_2$	1.44	7.2	4.5	2.5	9.3	1.395
$ScNi_2$			Pauli paramagnetic			1.384

Notes: The values of the characteristic temperatures were calculated to an accuracy of ±0.1 K, the values of the magnetic moments were calculated to an accuracy of ±0.01 μ_B, the values of the cell parameters were calculated to an accuracy of ±0.001 nm.

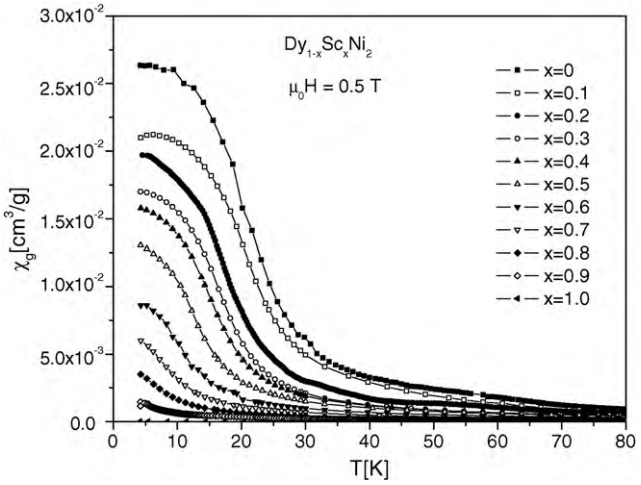

Fig. 2. Temperature dependence of the magnetic susceptibility of $Dy_{1-x}Sc_xNi_2$ (x = 0–1.0) solid solutions measured in 0.5 T at low-temperature region.

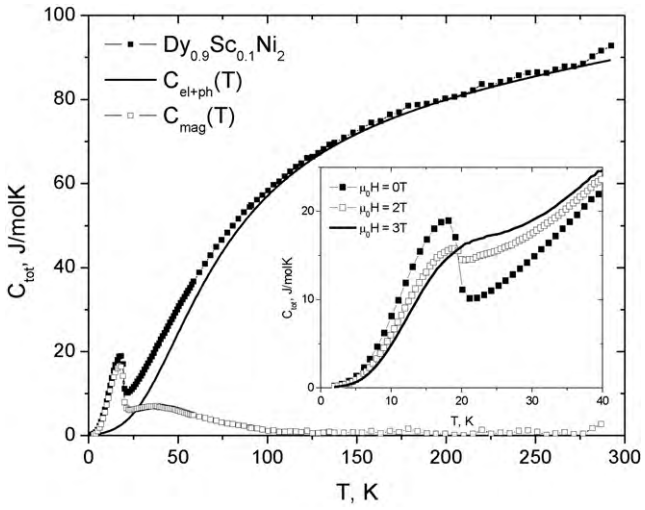

Fig. 3. The total heat capacity $C_{tot}(T)$ of $Dy_{0.9}Sc_{0.1}Ni_2$ in a zero magnetic field. The insets show a low-temperature portion of the $C_{tot}(T)$ curve in 0, 2 and 3 T.

dependence corresponding to the temperature-independent Pauli paramagnetism. At room temperature, the magnetic susceptibility of $ScNi_2$ is $\chi_g = 5.72 \times 10^{-6}$ cm^3/g.

The calculated values of the effective magnetic moment μ_{eff} per dysprosium atom for almost all the studied alloys are well below the value of 10.6 μ_B, which is expected for the pure Dy metal (Table 1). Only in the case of $DyNi_2$ and $Dy_{0.5}Sc_{0.5}Ni_2$ the effective magnetic moment is near that of Dy. The ferromagnetic Curie temperature T_C was estimated using the maximum in the $\delta\chi(T)/\delta T$ vs. T plots. The substitution of Sc for Dy in the $Dy_{1-x}Sc_xNi_2$ solid solutions leads to the decrease in the magnetic ordering temperature. Similar behavior was observed for the substitution of La for Dy in $Dy_{1-x}La_xNi_2$. However, the magnetic order is present in $Dy_{1-x}La_xNi_2$ for substitutions as high as 80% of nonmagnetic atoms [24].

3.4. Heat capacity

The results of heat capacity study in the solid solutions $Dy_{1-x}Sc_xNi_2$ are presented in Table 2. As an example the temperature dependencies of the heat capacity $C_{tot}(T)$, the sum of electron and phonon $C_{el+ph}(T)$ and magnetic contributions $C_{mag}(T)$ of solid solutions $Dy_{0.9}Sc_{0.1}Ni_2$ and $Dy_{0.5}Sc_{0.5}Ni_2$ measured in zero magnetic field are shown in Figs. 3 and 4, respectively. In the case of $Dy_{0.9}Sc_{0.1}Ni_2$ (Fig. 3), a well defined λ-like anomaly observed at 19.0 K and for $Dy_{0.5}Sc_{0.5}Ni_2$ a similar anomaly is observed at 10 K. The sharp λ-kind maxima on the heat capacity curves correspond to the temperature of the magnetic ordering. This shape of the anomalies is typical for a second order phase transition. The insets of Figs. 3 and 4 show the low-temperature variation of $C_{tot}(T)$ measured in zero, 2 and 3 T magnetic field. Heat capacity measurements in a magnetic field (insets in Figs. 3 and 4) show that the magnetic field causes the broadening and displacement of the maximum. The height of the maximum decreases with increasing magnetic field. The T_C values are summarized in Table 2 and are close to those evaluated from the magnetic measurements (Table 1).

The relatively low Curie temperature does not allow for an accurate determination of the electronic heat capacity coefficient γ and

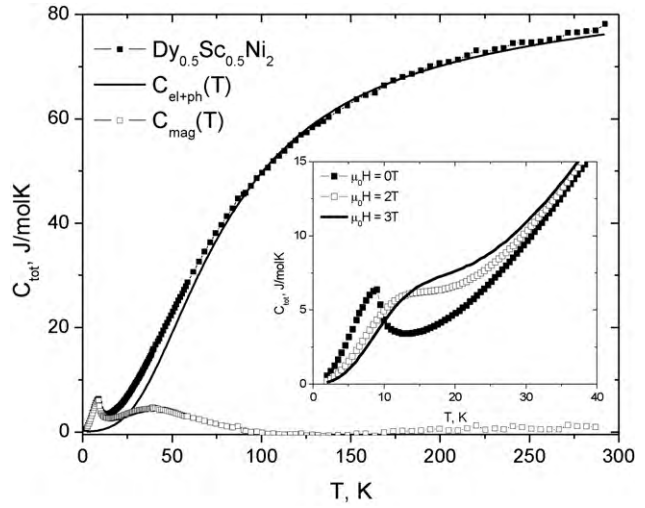

Fig. 4. The total heat capacity $C_{tot}(T)$ of $Dy_{0.5}Sc_{0.5}Ni_2$ measured in a zero magnetic field. The insets show a low-temperature portion of the $C_{tot}(T)$ curve measured in 0, 2 and 3 T.

Table 2
Physical properties for $Dy_{1-x}Sc_xNi_2$ solid solutions obtained from heat capacity data: T_C is Curie temperature, θ_D is Debye temperature (for γ = 17 mJ/mol K^2 as fixed parameters), ΔT_{ad} is adiabatic temperature change.

Compound	T_C (K)	θ_D (K)	ΔT_{ad} μ_0H = 1 T (K)	ΔT_{ad} μ_0H = 2 T (K)	ΔT_{ad} μ_0H = 3 T (K)
$DyNi_2$	21.2	250	–	–	–
$Dy_{0.9}Sc_{0.1}Ni_2$	19.6	290	2.8	4.9	6.7
$Dy_{0.8}Sc_{0.2}Ni_2$	17.5	300	–	–	–
$Dy_{0.7}Sc_{0.3}Ni_2$	16.3	305	2.4	–	–
$Dy_{0.6}Sc_{0.4}Ni_2$	13.2	310	–	–	–
$Dy_{0.5}Sc_{0.5}Ni_2$	10.2	315	2.6	4.8	7.1
$Dy_{0.4}Sc_{0.6}Ni_2$	6.1	319	1.9	3.6	–
$Dy_{0.3}Sc_{0.7}Ni_2$	5.0	320	1.3	2.9	–
$Dy_{0.2}Sc_{0.8}Ni_2$	4.5	322	–	–	–

Note: The values of the characteristic temperatures were calculated to an accuracy of ±0.1 K.

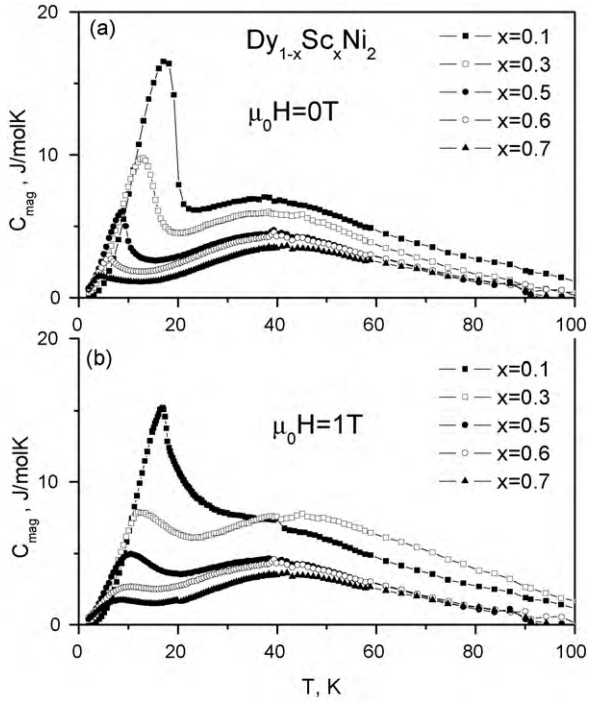

Fig. 5. The low-temperature (below 100 K) magnetic part of heat capacity C_{mag} vs. T dependence of the $Dy_{1-x}Sc_xNi_2$ solid solutions in 0 T (a) and 1 T (b).

Debye temperature Θ_D in the low-temperature range. In order to estimate the magnetic contribution a theoretical calculation of the Debye function was made [25]. The Debye temperatures and γ values were calculated using the Debye function in the temperature range of 2–300 K and are shown in Table 2. The best fit for the wide temperature range could be obtained by fixing the parameters γ = 17 mJ/mol K^2 for all the measured samples, while the Debye temperature was increased as the Sc content increases, similarly to the $Ho_{1-x}Sc_xNi_2$ system [26].

Fig. 5 shows the magnetic part of the heat capacity of the $Dy_{1-x}Sc_xNi_2$ solid solutions (x = 0.1, 0.3, 0.5, 0.6, 0.7) measured in zero (Fig. 5a) and in an external magnetic field of 1 T (Fig. 5b).

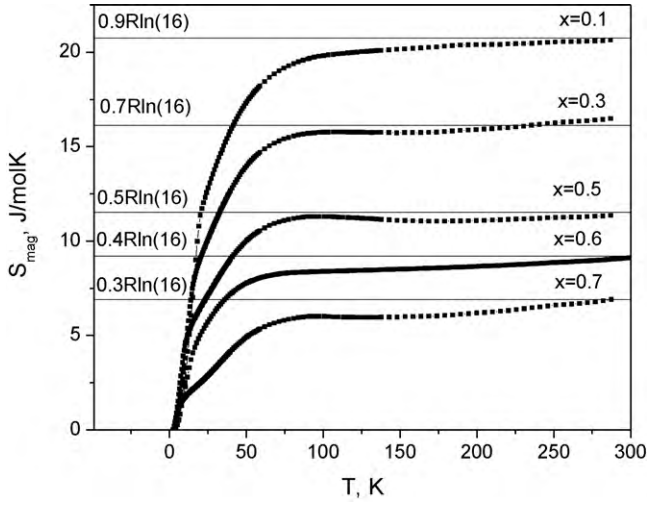

Fig. 6. Magnetic part of the entropy S_{mag} of $Dy_{1-x}Sc_xNi_2$ (x = 0, 0.3, 0.5, 0.6, 0.7) in 0 T. The dotted lines indicate the (1−x)Rln(16) limits.

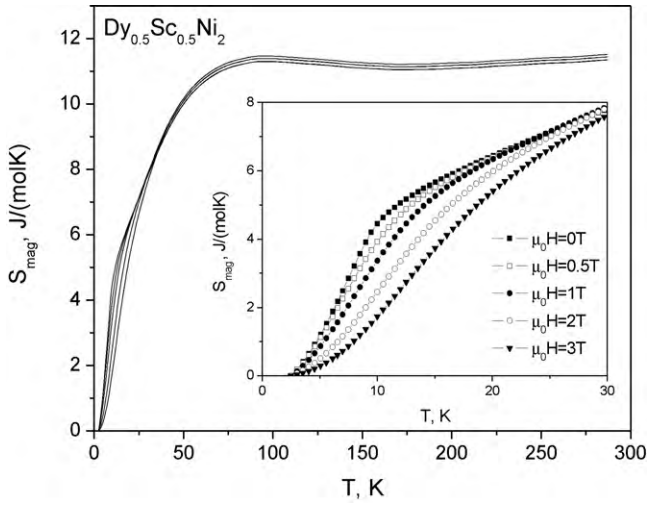

Fig. 7. Magnetic part of the entropy S_{mag} of $Dy_{0.5}Sc_{0.5}Ni_2$ 0, 0.5, 1, 2 and 3 T. The insets show a low-temperature region.

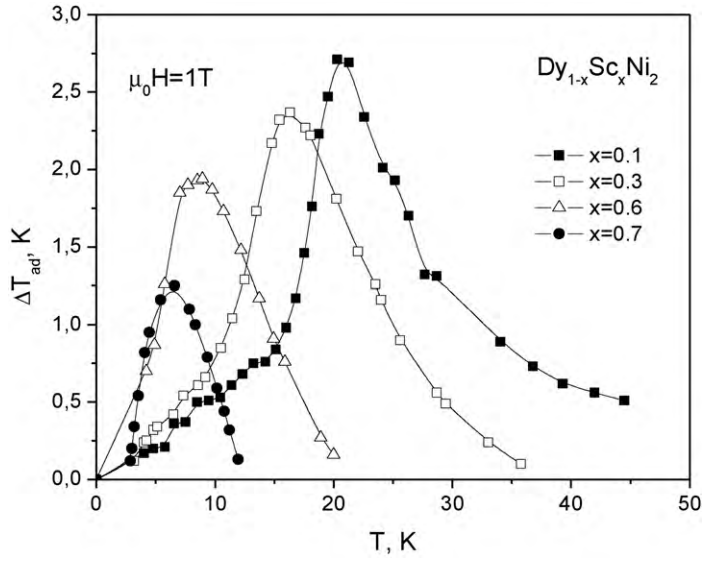

Fig. 8. Temperature dependence of ΔT_{ad} of $Dy_{1-x}Sc_xNi_2$ (x = 0.1, 0.3, 0.6, 0.7) for a magnetic field change of 1 T.

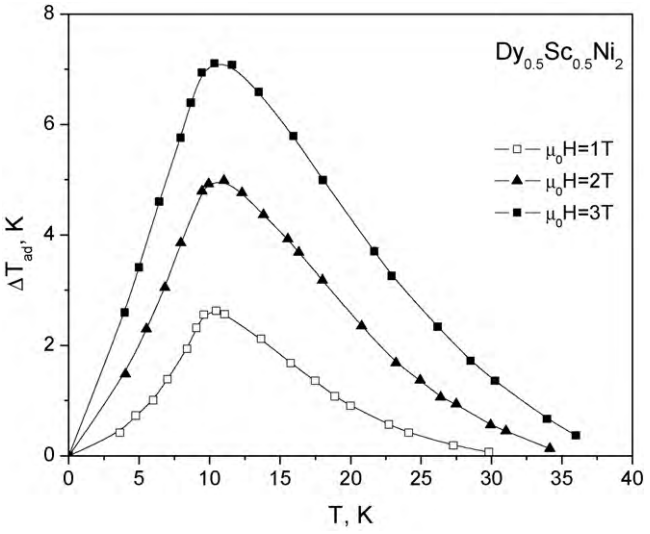

Fig. 9. Temperature dependence of ΔT_{ad} of $Dy_{0.5}Sc_{0.5}Ni_2$ for a magnetic field change of 1, 2 and 3 T.

A maximum is observed in the vicinity of the Curie temperature. For the solid solutions with $x = 0.1$, 0.3, 0.5, 0.6 and 0.7, the maxima are observed at 19, 16, 10, 6 and 5 K, respectively. Similarly to $C_{tot}(T)$, the height of the magnetic part of the heat capacity is reduced in the presence of the magnetic field. In the paramagnetic regime, a broad maximum has been observed, which apparently corresponds to the Schottky anomaly that is caused by a crystal field splitting of the Dy^{3+} ground-state level. The Dy ions have a large orbital moment $L = 5$ and, therefore, not only the low symmetry but also the local anisotropy of Dy ions gives rise to the crystal field (CF) effect.

The magnetic part of the entropy S_{mag} was calculated by integrating $C_{mag}(T)/T$. S_{mag} for $x = 0.1$, 0.3, 0.5, 0.6 and 0.7 solid solutions in a zero magnetic field is shown in Fig. 6. The magnetic entropy does not reach the theoretical maximum values $S_{max} = R\ln(16)$ in the low-temperature region and approaches the theoretical value near 300 K. This behavior of the magnetic entropy can be explained by peculiarities in the ground-state level splitting by crystal field.

Fig. 7 shows the temperature variation of the magnetic entropy in zero, 0.5, 1, 2 and 3 T magnetic fields for $Dy_{0.5}Sc_{0.5}Ni_2$. S_{mag} increases with increasing temperature and, as expected, the application of the magnetic field leads to the decrease of S_{mag} in the vicinity of T_C.

The adiabatic temperature change ΔT_{ad} was calculated using a formula suggested by von Ranke et al. [2]. The temperature dependence of ΔT_{ad} of $Dy_{1-x}Sc_xNi_2$ for $x = 0.1$, 0.3, 0.6 and 0.7 near its ordering temperature under 1 T magnetic field is shown in Fig. 8. The maximum peak value decreases with increasing Sc content. As an example the temperature dependence $\Delta T_{ad}(T)$ of $Dy_{0.5}Sc_{0.5}Ni_2$ solid solution measured in 1, 2 and 3 T magnetic field is shown in Fig. 9. As expected, the magnetic field leads to an increase of ΔT_{ad}. Moreover the temperature range over which the MCE is considerable is wide, which is essential for a practical magnetic refrigerant. The sharp peaks in the ΔT_{ad} curves are related to the paramagnetic–ferromagnetic phase transition at the Curie point, where the magnetization change is maximal.

4. Conclusion

The analysis of the structural data confirms that $Dy_{1-x}Sc_xNi_2$ alloys crystallize with in a cubic C15 structure (space group $F\bar{4}3m$), which is a derivative of the C15-type structure (space group Fd3m) with a doubled lattice parameter.

The substitution of Sc for Dy atoms markedly modifies the magnetic behavior of the $Dy_{1-x}Sc_xNi_2$ alloys. The replacement of the magnetic Dy by the nonmagnetic Sc results in a common magnetic dilution leading to a weakening of the exchange interactions and to the decrease of the ordering temperature. The magnetic moment, Curie and Debye temperatures are reduced as the Sc content increases to $x = 0.8$. The Curie temperature decreases linearly from 21.3 K for $DyNi_2$ to 4.5 K for $Dy_{0.2}Sc_{0.8}Ni_2$.

The Debye temperatures estimated from the Debye function in the temperature range of 2–300 K increase from 250 K for $DyNi_2$ to 322 K for $Dy_{0.2}Sc_{0.8}Ni_2$ with increasing Sc content. The magnetic part of the heat capacity showed the presence of the Schottky anomaly phenomenon.

The maximum MCE estimated for $Dy_{0.9}Sc_{0.1}Ni_2$ and $Dy_{0.5}Sc_{0.5}Ni_2$ reaches about 7 K for a field change of 3 T at around 19 and 10 K, respectively. The large MCE at low temperatures implies that $Dy_{1-x}Sc_xNi_2$ is a possible magnetic refrigerant candidate for hydrogen liquefaction.

References

[1] V.K. Pecharsky, K.A. Gschneidner Jr., Phys. Rev. Lett. 78 (1997) 4494.
[2] P.J. von Ranke, D.F. Grangera, A. Caladas, N.A. de Olivera, J. Appl. Phys. 93 (2003) 4055.
[3] N.H. Duc, D.T. Kim Anh, P.E. Brommer, Physica B 319 (2001) 1.
[4] N.V. Tristan, S.A. Nikitin, T. Palewski, K. Nenkov, K. Skokov, J. Magn. Magn. Mater. 258 (2003) 583.
[5] K.A. Gschneidner, V.K. Pecharsky, S.K. Malik, Adv. Cryog. Eng. 42A (1997) 475.
[6] N.K. Singh, K.G. Suresh, A.K. Nigam, Solid State Commun. 127 (2003) 373.
[7] N.K. Singh, S.K. Tripathy, D. Banerjee, C.V. Tomy, K.G. Suresh, A.K. Nigam, J. Appl. Phys. 95 (2004) 6678.
[8] J. Lyubina, O. Gutfleisch, M.D. Kuzmin, M. Richter, J. Magn. Magn. Mater. 320 (2008) 2252.
[9] J. Lyubina, K. Nenkov, L. Schultz, O. Gutfleisch, Phys. Rev. Lett. 101 (2008) 177203.
[10] A. Yan, K.H. Müller, L. Schultz, O. Gutfleisch, J. Appl. Phys. 99 (2006), 08K903, 1.
[11] W.E. Wallace, E. Segal, in: A.M. Alper, J.L. Margrave, A.S. Nowick (Eds.), Rare Earth Intermetallics, Academic Press, New York, 1973.
[12] K.H.J. Buschow, in: E.P. Wohlfarth (Ed.), Ferromagnetic Materials, vol. 1, North Holland, Amsterdam, 1980.
[13] R. Malik, P.L. Paulose, E.V. Sampathkumatan, S. Patil, V. Nagarajan, Phys. Rev. B 55 (1997) 8369.
[14] M. Mizumaki, K. Yano, I. Umehara, F. Ishikawa, K. Sato, N. Sakai, T. Muro, Phys. Rev. B 67 (2003) 132404.
[15] E.A. Skrabek, W.E. Wallace, J. Appl. Phys. 34 (1963) 1356.
[16] M.R. Ibarra, J.I. Arnaudas, P.A. Algarabel, A. del Moral, J. Magn. Magn. Mater. 46 (1984) 167.
[17] A.S. Markosyan, Fiz. Tverd. Tela 23 (1981) 1153.
[18] J. Ćwik, T. Palewski, G.S. Burkhanov, O.D. Chistyakov, K. Nenkov, Phys. Status Solidi A 201 (3) (2004) 445.
[19] H.R. Kirchmayer, E. Burzo, in: H.P.J. Wijn (Ed.), Landolt-Börnstein, New Series III/19d2, Berlin, 1990.
[20] M. Latroche, V. Paul-Boncour, A. Percheron-Guegan, Z. Phys. Chem. 179 (1993) 262.
[21] A. Lindbaum, J. Hafner, E. Gratz, J. Phys.: Condens. Matter 11 (1999) 1177.
[22] E. Dormann, K.H.J. Buschow, Physica 86–88B (1977) 75.
[23] E. Burzo, J. Laforest, Intern. J. Magn. 3 (1972) 171.
[24] J. Ćwik, T. Palewski, K. Nenkov, J. Lyubina, J. Warchulska, J. Klamut, O. Gutfleisch, J. Magn. Magn. Mater. 321 (2009) 2821.
[25] M. Bouvier, P. Lethuillier, D. Schmitt, Phys. Rev. 43 (1991) 13137.
[26] J. Ćwik, T. Palewski, K. Nenkov, G.S. Burkhanov, O.D. Chistyakov, J. Warchulska, Phys. Status Solidi B 242/10 (2005) 1969.